Impact of convection on three dimensional Casson rotatory fluid over an extending sheet: A numerical approach

Alfunsa Prathiba[1,*], A. Venkata Lakshimi[2]

[1]Department of Mathematics, CVR College of Engineering, Telangana 501510, India
[2]Associate Professor of Mathematics, Department of Mathematics, Osmania University, Hyderabad, 007, India.

ABSTRACT

Natural convection occurs in fluid environments. Usually, it is facilitated by the buoyancy effect. It is significantly less efficient than forced convection, due to the lack of fluid motion. As a result, it is completely dependent on the buoyancy effect's strength and the fluid's viscosity. The current work investigates the convective flow of a three-dimensional Casson fluid across a rotating linear expanding sheet. The nonlinear governing equations of the steady flow were presented and reconstructed using appropriate similarity transformations. To solve the resultant equations, the three-stage collocation approach namely Lobatto IIIA was applied using MATLAB. Graphs were used to illustrate the physical properties of the required data. It was observed that while the primary velocity profile decreases as the Casson, convective, and rotational parameters increase, the secondary velocity profile exhibits the opposite behaviour. The effect of rotation, Casson parameter, and others on drag coefficient, heat transfer coefficient, and mass transfer coefficient was evaluated, interpreted, and found to be reasonably consistent with earlier research.

Keywords: Rotating fluid; 3-D Casson fluid; Lobatto IIIA collocation method**.**
DOI: https://dx.doi.org/10.4314/ejst.v15i3.7

INTRODUCTION

The researchers looked at how heat transfer and concentration convections in the boundary layer flow over an extending surface with constant but varying temperatures and concentrations at the edges (Rashid *et al*., 2019). Flows like these can be found in various engineering, geophysical, and storage systems applications. When heat transfer occurs over a changing surface, the majority of the difficulties are generated by boundary displacement and buoyancy effects. A few instances of this type of flow include solar collectors exposed to the wind, computer devices

*Corresponding Author: alphonsaperli@gmail.com
©This is an Open Access article distributed under the terms of the Creative Commons Attribution License (http://creativecommons.org/licenses/CC BY4.0)

cooled by fans, and nuclear power facilities cooled by blowers when they experience an unexpected breakdown (Bilal Ashraf *et al*., 2017). M. Bilal Ashraf *et al*. (Bilal Ashraf *et al*., 2017) analysed the effects of the hall effect and convective boundary conditions on the mixed natural convection with the use of a series solution. In their study, they found that Transversal velocity increases as Hartman number M. An electrically conducting incompressible fluid through a vertical porous channel filled with porous materials, and the impacts of magnetic field, permeability of porous, suction/injection, materials, and viscous dissipation were investigated theoretically by Ajibade *et al*. (Ajibade *et al*., 2021). Seghir-Ouali *et al*. (Seghir-Ouali *et al*., 2006) developed an experimental detection procedure for the convective heat transfer coefficient within a rotating cylinder with an axial airflow for various rotational speeds corresponding to varied rotational Reynolds numbers and an airflow rate. Some significant findings of natural and mixed convection can be noticed in the references (Nadeem & Saleem, 2014a; Gangaiah *et al*., 2019; Ghosh and Mukhopadhyay, 2020; Malaver *et al*., 2020; Rajesh *et al*., 2020; Islam *et al*., 2021; Prathiba & Akavaram, 2022).

The investigation of rotational fluid surge, which originates from the "*Coriolis force"*, has important applications in geophysical situations, astrophysics, oceanography, and other fields. Moreover, this type of flow across a stretched plane is used in various industries, including yarn spinning, plastic sheet extrusion, food processing, and glass wafting (Archana *et al*., 2018). Rotating flows are also used in geotechnical engineering for the fields such as centrifugal purification, turbines, material treating, and rotatory hydromagnetic generators (Shanker Seth and Kumar Mandal, 2018). Wang (Wang, 1988) investigated the rotating fluid flow problem using a two-dimensional stretchable surface. Furthermore, when the rotation parameter was larger than unity, he acquired a more precise solution employing the analytic approach than the numerical approach. Several scholars looked into the peculiarities of flow behaviour when rotation was taken into account (Nadeem & Saleem, 2014b; Qayyum *et al*., 2018; Shanker Seth & Kumar Mandal, 2018; Ali *et al*., 2020; Anuar *et al*., 2020; Ijaz Khan *et al*., 2020; Salahuddin *et al*., 2020; Hussain *et al*., 2021; Krishna *et al*., 2021; Shoaib *et al*., 2021).

Fluids are necessary for existence, and scientists have uncovered many statistics and illustrations about fluid movement due to their importance in natural and industrial processes. Fluid dynamics is the study of fluid flow and how forces affect it. Using an approach, it demonstrates how to explain star evolution, weather phenomena, sea currents, and blood circulation. "Archimedes was a Greek mathematician" who studied the buoyancy and statics of fluids before formulating the Archimedes principle, considered the earliest contribution to fluid mechanics. In the fourteenth century, a flurry of research into this topic began (Narender *et al*., 2021). Many fluids in nature display a nonlinear connection between stress and distortion rate and are referred to as non-Newtonian fluids (NNF). Because of their extensive

applicability in fields such as unrefined oil withdrawal from gasoline fuels, food production, paper, and fibre lamination, several scientists were interested in investigating the phenomena of movement of these types of fluids. Because of the diversity of NNF, no single constitutive equation can adequately describe their properties. So, different models for such types of fluids have been devised (Archana *et al*., 2018). Casson fluid is one such NNF containing properties such as human blood, jellies, nectar, juice with fibres, etc. Fluids with this nature could be useful in medicinal and industrial fields. Casson fluid is a shear-thinning fluid with infinite viscosity at zero shear rate, yield stress below which no flow occurs, and zero viscosity at the infinite shear rate (Dash *et al*., 1996; Ali *et al*., 2020). Numerous researchers have investigated Casson fluid's movement and heat transfer characteristics from different physical and mathematical perspectives (Reza *et al*., 2016; Besthapu *et al*., 2019; Raju & Mallikarjuna, 2019; Salahuddin *et al*., 2020; Mangathai *et al*., 2021; Sahoo & Nandkeolyar, 2021; Satya Narayana *et al*., 2021).

Rotation is critical in managing up and down heat and mass transfer phenomena in manufacturing and industrial relevance. The above stated analysis discloses that the effect of convection on a rotating Casson fluid flow was not addressed extensively. The above. Our intention thus here employs the motivations of the previous studies to explore the heat and mass transfer characteristics of Casson linear flow across a spinning sheet in the existence of natural convection. The developed set of linked non-linear governing equations was numerically solved using the Lobatto IIIA method (Shoaib *et al*., 2020; Umar *et al*., 2020; Ahmad *et al*., 2021; Alhamaly *et al*., 2021; Lund *et al*., 2021a; Lund *et al*., 2021b; Prathiba and Akavaram, 2022). BVP4C implements the three-stage Lobatto IIIa formula in MATLAB, a finite difference code.

"Mesh selection and error control are based on the continuous solution's residual (http://www.mathworks.com/help/matlab/ref/bvp4c.html#moreabout). Graphs and tables depict the effect of flow control parameters on velocity, temperature, and concentration fields and the skin friction coefficient, heat, and mass transfer rate".

FORMULATION OF THE PROBLEM

Considering a three-dimensional steady, incompressible boundary layer flow (BLF) of a three-dimensional Casson fluid stimulated by the stretching of a heated surface. The flow is assumed to flow over xy-plane with the velocity components in the (x, y, z) direction given as (u, v, w). Also, the axis of rotation being considered in z-direction with angular velocity Ω' .The surface is assumed to be stretching at a rate proportionate to its distance from the origin in the x-direction. The temperature of the stretching surface is held constant at T_w, while the temperature of the distant fluid is presumed to be T_∞.

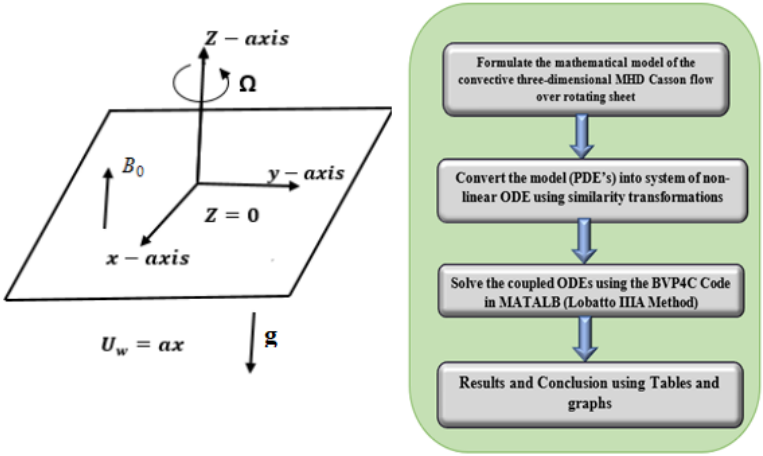

Figure 1. Sketch and Scheme of the problem

Casson fluid has a rheological model that is described as(Archana *et al*., 2018),

$$\tau_{ij} = \begin{cases} 2\left(\mu_B + \dfrac{p_y}{\sqrt{2\pi}}\right)e_{ij}, & \pi > \pi_c \\ 2\left(\mu_B + \dfrac{p_y}{\sqrt{2\pi_c}}\right)e_{ij}, & \pi < \pi_c \end{cases}, \quad (1)$$

Where τ_{ij} is the "*Cauchy stress tensor*", $\pi = (e_{ij})^2$ is "the product of deformation rate" components with itself, e_{ij} is the $(i,j)^{th}$ deformation rate constituent, π_c is the "critical value" of a product based on the non-Newtonian model, $\mu_B$is the non-Newtonian model plastic dynamic viscosity, and p_y is the fluid yield stress (Butt *et al*., 2015). s

Currently, $\tau_{xz} = \mu_B\left(1+\dfrac{1}{\beta^{\cdot}}\right)\left(\dfrac{\partial w}{\partial x}+\dfrac{\partial u}{\partial z}\right)$ *and* $\dfrac{\partial w}{\partial x}=0$ *where* $\beta^{\cdot} = \mu_B\dfrac{\sqrt{2\pi_c}}{p_y}$ is the Casson fluid parameter.

Implementing the above constraints, the regulating equations for the continuity, momentum and energy, mass diffusion are (Butt *et al*., 2015; Shanker Seth and Kumar Mandal, 2018; Senapati *et al*., 2020):

$$\frac{\partial u}{\partial x}+\frac{\partial v}{\partial y}+\frac{\partial w}{\partial z}=0 \tag{2}$$

$$u\frac{\partial u}{\partial x}+v\frac{\partial u}{\partial y}+w\frac{\partial u}{\partial z}-2\Omega' v=\vartheta\left\{1+\frac{1}{\beta}\right\}\frac{\partial^2 u}{\partial z^2}-\frac{\sigma}{\rho}B_0^2 u+g\left(\beta_T\left(T-T_\infty\right)+\beta_c\left(C-C_\infty\right)\right) \tag{3}$$

$$u\frac{\partial v}{\partial x}+v\frac{\partial v}{\partial y}+w\frac{\partial v}{\partial z}+2\Omega' u=\vartheta\left\{1+\frac{1}{\beta}\right\}\frac{\partial^2 v}{\partial z^2}-\frac{\sigma}{\rho}B_0^2 v \tag{4}$$

$$u\frac{\partial T}{\partial x}+v\frac{\partial T}{\partial y}+w\frac{\partial T}{\partial z}=\alpha\frac{\partial^2 T}{\partial z^2} \tag{5}$$

$$u\frac{\partial C}{\partial x}+v\frac{\partial C}{\partial y}+w\frac{\partial C}{\partial z}=D_M\frac{\partial^2 C}{\partial z^2} \tag{6}$$

The presumed boundary conditions are(Bilal Ashraf *et al*., 2017),

$$u = U_w = \hat{a}x, v = 0, w = 0, T = T_w, C = C_w \text{ at } z = 0$$
$$u \to 0, v \to 0, w \to 0, T \to T_\infty, C \to C_\infty \text{ at } z \to \infty \tag{7}$$

where, (ρ) fluid density, (ϑ) is the "kinematic viscosity"′, (σ) "electrical conductivity", Casson parameter (β) , β_T is the thermal expansion coefficient, β_C is the solutal expansion coefficient, fluid temperature(T), free stream temperature (T_∞), g is the "gravity acceleration", (α) "thermal diffusivity", (C_p) "specific heat at constant pressure", and â >0 constant, (D_M) Molecular Diffusivity coefficient, (C) concentration of the species.

The transformation variables are stated as follows(Anuar *et al*., 2020)

$$\eta=\sqrt{\frac{\hat{a}}{\vartheta}}z, u=\hat{a}xF'(\eta), v=\hat{a}xG(\eta), w=\sqrt{\hat{a}\vartheta}F(\eta), \theta(\eta)=\frac{T-T_\infty}{T_w-T_\infty}, \varphi(\eta)=\frac{C-C_\infty}{C_w-C_\infty} \tag{8}$$

Equation (2) is satisfied by the above transformations, and equations (3) – (6) reduce to the following "self-similar ordinary differential equations":

$$\left(1+\frac{1}{\beta}\right)F'''-M^*F'-\left(F'\right)^2+F''F+2\omega G+\lambda^*\left(\theta+N_1^*\varphi\right)=0 \tag{9}$$

$$\left(1+\frac{1}{\beta}\right)G''-M^*G-\left(F'G-G'F\right)-2\omega F'=0 \tag{10}$$

$$\theta'' + Pr\cdot F\theta' = 0 \tag{11}$$

$$\varphi'' + Sc.F\varphi' = 0 \tag{12}$$

The comprehensive boundary constraints are attained as:

$$\left.\begin{aligned} &F'(\eta)=1, G(\eta)=0, F(\eta)=0, \theta(\eta)=1, \varphi(\eta)=1 \quad at \ \ \eta=0 \\ &F'(\eta)\to 0, G(\eta)\to 0, \theta(\eta)\to 0, \varphi(\eta)\to 0 \quad as\ \eta\to\infty \end{aligned}\right\} \tag{13}$$

The parameters in the above equations are given as Magnetic parameter ($M^* = \sigma.B_0^2/\rho$â), Rotation parameter (ω=Ω/â), Prandtl Number ($Pr\cdot = \vartheta/\alpha$), Schmidt Number ($Sc = \vartheta/D_M$), the combined convection parameter (Zaigham Zia *et al*., 2018) ($\lambda^* = {Gr}/{Re_x^2}$) ,the Buoyancy ratio parameter (Zaigham Zia *et al*., 2018)

$\left(N_1^* = {\beta_c(C_w - C_\infty)}/{\beta_T(T_w - T_\infty)} \right)$, "Grashof Number"

($Gr = g\beta_T(T_w - T_\infty)x^3/\vartheta^2$) .

The physical quantities of engineering purposes i.e., the drag friction coefficients C_{fx} *and* C_{fy}, the diminished Nusselt number, and Sh_x(the Sherwood number), are as follows.

$$C_{fx} = \left(1+\frac{1}{\beta\cdot}\right)F''(0), C_{fy} = \left(1+\frac{1}{\beta\cdot}\right)G'(0), Re_x^{-1/2}\, Nu_x = -\theta'(0), Re_x^{-1/2}\, Sh_x = -\varphi'(0),$$

$$Re_x = {U_w x}/{\vartheta}\ (local\ Re\ ynold's\ Number)$$

NUMERICAL SOLUTION

The system of coupled dimensionless Equations (9)– (12) is sensitive to boundary conditions mathematically. Since these equations are highly nonlinear, solving them analytically is quite challenging. As a result, the BVP4C approach from MATLAB is one of the methods utilised to solve such problems. The numerical solutions are acquired utilising the MATLAB BVP algorithm bvp4c, "a finite difference code that implements the three-stage Lobatto IIIA formula".

In this procedure, the above equations are first metamorphosed into a set of "coupled first-order equations" as follows:

$$\begin{aligned} f &= \left[F\ F'\ F''\ \ G\ G'\ \theta\ \theta'\ \varphi\ \varphi' \right]^T \\ &= \left[f(1)\ f(2)\ f(3)\ f(4)\ f(5)\ f(6)\ f(7)\ f(8)\ f(9) \right]^T \end{aligned} \tag{14}$$

Therefore, the equations (9) - (12) can be expressed as:

$$\frac{d}{d\eta}\begin{bmatrix} f(1) \\ f(2) \\ f(3) \\ f(4) \\ f(5) \\ f(6) \\ f(7) \\ f(8) \\ f(9) \end{bmatrix} = \begin{bmatrix} f(2) \\ f(3) \\ \dfrac{\left(M^*\right) f(2) + f(2)\wedge 2 - f(2) f(1) - 2\omega f(4) - \lambda^*\left(f(6) + N_1^* f(8)\right)}{\left(1+\dfrac{1}{\beta}\right)} \\ f(5) \\ \dfrac{\left(M^*\right) f(4) + f(2) f(4) - f(5) f(1) + 2\omega f(2)}{\left(1+\dfrac{1}{\beta}\right)} \\ f(7) \\ -Pr\left\{f(1) f(7)\right\} \\ f(9) \\ -Sc\ f(1) f(9) \end{bmatrix}$$

This is put up as a "boundary value problem (BVP)" in MATLAB, and the Lobatto IIIA RK collocation method is used to derive the solution of the system of equations along with the required boundary conditions (BVP4C). When the error (tolerance) reaches 10^{-6}, the procedure will be terminated. When solving the BVP using MATLAB, Bvp4c requires only three arguments: a "functionode" for evaluating the ODEs, a "functionbc" for evaluating the residual in the boundary conditions, and a "solinit" structure for generating an approximation for a mesh and the solution on this mesh. The ODEs are computed in almost the same approach as the IVP solvers in MATLAB (Prathiba & Akavaram, 2022). This method can be explained by various research articles (Ibrahim, 2017; Uddin *et al*., 2019; Ouyang *et al*., 2020; Ahmad *et al*., 2021; Shoaib *et al*., 2021; Vedavathi *et al*., 2021).

DISCUSSION OF THE RESULTS OBTAINED

The non-linear differential equations of the MHD Casson fluid with viscous dissipation over a rotating sheet and the boundary conditions were solved using the 3-stage Lobatto IIIA R.K collocation method. The technique was implemented using the symbolic software MATLAB. The boundary conditions defined at infinity are switched by a sufficiently substantial value $\eta = \eta_{max} = 10$. The accuracy of up to six decimal places has been considered for the convergence criteria with a step size of $\Delta\,\eta = 0.001$. The code validation was done by comparing the values of physical interest, such as drag friction coefficient, with Wang (Wang, 1988) and Adnan Saeed *et al*. (Butt *et al*., 2015) (Table 1).

Table 1. Validation of code by taking when N_1^*=Sc=M^*= λ^*=0, $\beta \to \infty$ comparing the current findings to previously computed results.

ω'	Wang C. Y (Wang, 1988)		Adnan Saeed Butt *et al.* (Butt *et al.*, 2015)		Present Results	
	$-F''(0)$	$-G'(0)$	$-F''(0)$	$-G'(0)$	$-F''(0)$	$-G'(0)$
0	1	0	1	0	1.000008	0
0.5	1.1384	0.5128	1.13838096	0.51276039	1.1383812	0.51276012
1	1.3250	0.8371	1.32502883	0.83709841	1.32502901	0.83709845
2	1.6523	1.2873	1.65235799	1.28725883	1.65235488	1.28725663

To study the performance of velocity, temperature, and concentration boundary layers, each parameter is graphically developed by assigning constant values to the parameters in the range mentioned below. The choices of the regulating parameters are the "Casson parameter" ($0.5 \leq \beta' \leq \infty$), rotation parameter ($0.2 \leq \omega' \leq 2$), the mixed convection parameter ($0 \leq \lambda^* \leq 2$), and the "Schmidt number" ($0< Sc<5$), the Buoyancy ratio ($0 \leq N_1^* \leq 2$) (The values of these parameters have been taken from the cited literature). As, the Prandtl number (Pr), can be defined as the ratio of molecular diffusivity of momentum to molecular diffusivity of heat and for a valid thermal analysis, in this analysis we have fixed the Pr at 6.20.

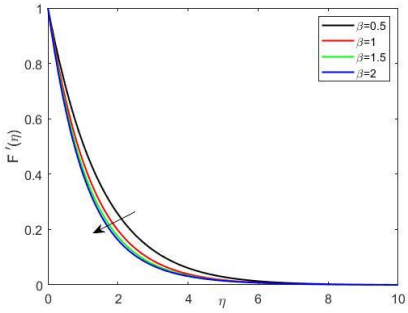

Figure 2.Performance of $F'(\eta)$ with β

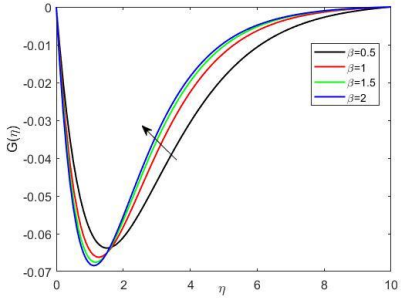

Figure 3 Impact of Casson Parameter β on G(η)

The influence of the Casson parameter on the PVG and SVG is seen in Figure 2 and Figure *3*. The velocity profiles F' drop as the value of β' increase and the SVG increase with rise in Casson parameter values. This is because tensile tension in the fluid flow due to elasticity generates resistance, resulting in a drop in primary velocity. As β' grows, the width of the velocity boundary layer decreases. On the other hand, increasing β', causes a fall in temperature profile and rise in concentration profile, as seen in Figure 4 and Figure *5*.

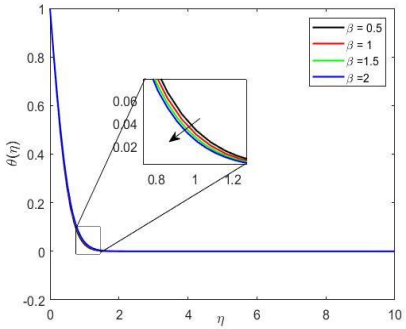

Figure 4 . Impact of Casson parameter on $\theta(\eta)$

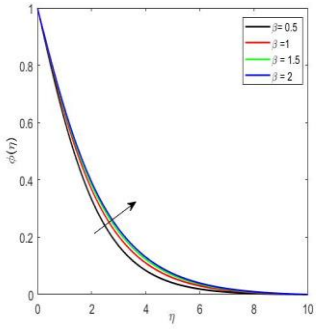

Figure 5 Impact of Casson parameter on ϕ(η)

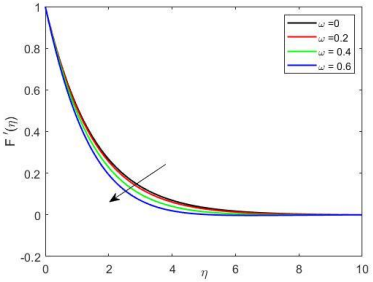

Figure 6 Influence of Rotational parameter on F´(η)

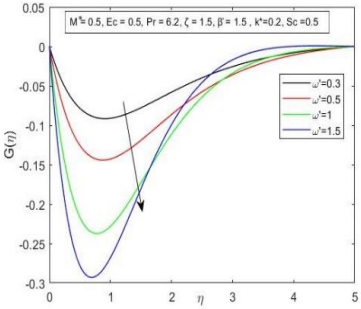

Figure 7 Influence of Rotational parameter on G(η)

Lower velocity dispersion is associated with higher rotation parameter values (Figure 6). The "Rotation Parameter (R.P)" is defined as the "ratio of rotation to stretching rates" in physical terms. Increased R.P values result in a faster rotational rate, causing the PVG velocity dispersion and the diameter of the momentum layer to decrease. The influence of the rotation parameter on the velocity distribution G is seen in Figure 7. This implies that rotation tends to accelerate secondary velocity whereas it retards primary velocity in the boundary layer region Thus, when the rotation parameter rises, the velocity distribution oscillates and also the mass diffusion.

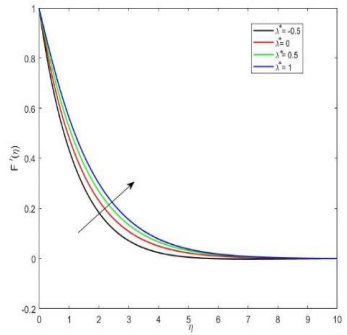

Figure 8. Effect of λ^* on PVG

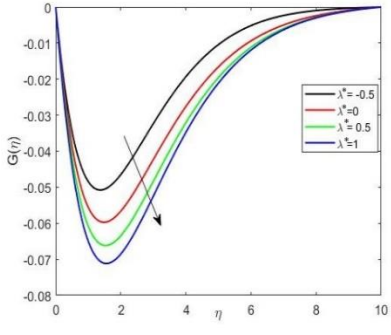

Figure 9. Effect of λ^* on SVG

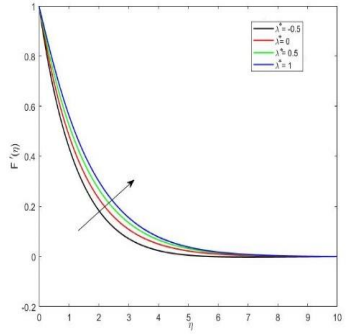

Figure 8. Effect of λ^* on PVG

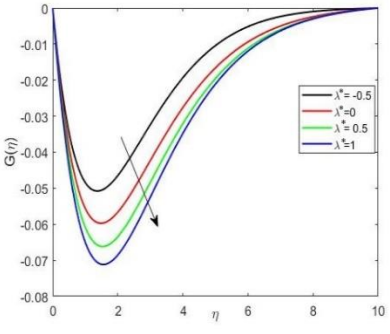

Figure 9. Effect of λ^* on SVG

Figures 8 and 9 show the effect of λ* on PVG and SVG. It is clear that F' is behaving increasingly, but G behaves in an opposing manner since, the positive buoyancy force ($\lambda^* > 0$) implies favourable pressure gradient, the fluid gets accelerated, which results in thinner momentum.

Figure 10 shows the attributes of N_1^* on PVG. N_1^* improves both velocity and boundary layer thickness in this case. The thermal expansion was dominated by concentration expansion, resulting in the rise in PVG. The presence of Lorentz force occurs due to the induced magnetic field resulting in decrease in primary velocity and increase in secondary velocity profiles. Also, the improvement in the magnetic parameter results in the enhancement of both temperature and concentration profiles, as seen in Figures 11 and 12.

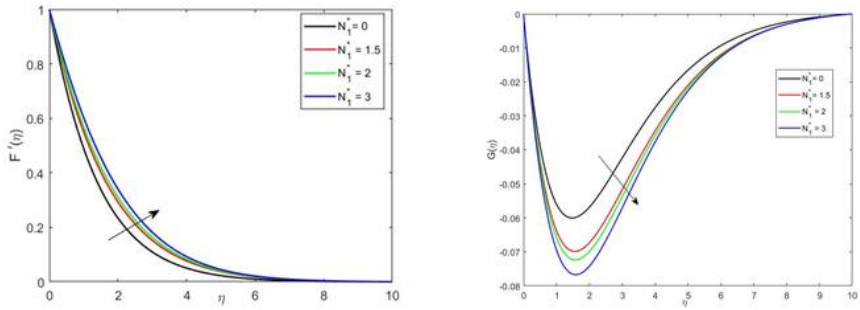

Figure 10. Influence of N_1^* on $F'(\eta)$ *and* G(η)

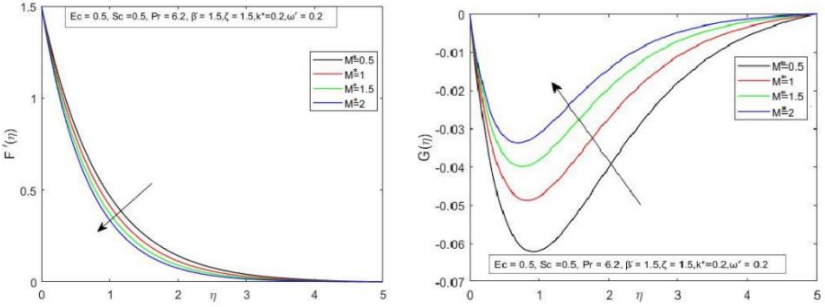

Figure 11. Effect of magnetic parameter on both primary and secondary velocity profiles

Table 2 shows the drag frictions' numerical results, which are important emerging parameters. Skin friction decreases in the x-direction for N_1^*, β, λ^*, but increases for M^*, Sc and R.P. We also noticed that skin friction in the y-direction increases as N_1^*, ω', λ^* increases but decreases as Sc, M^*, β increases. Sherwood numerals correspond to different N_1^*, ω', λ^*, Sc values. We concluded that for λ^*, N_1^*, the estimations of Nusselt and Sherwood numbers are improved. However, for Sc, the opposite impact is observed on N_{ux} *and* Sh_x.

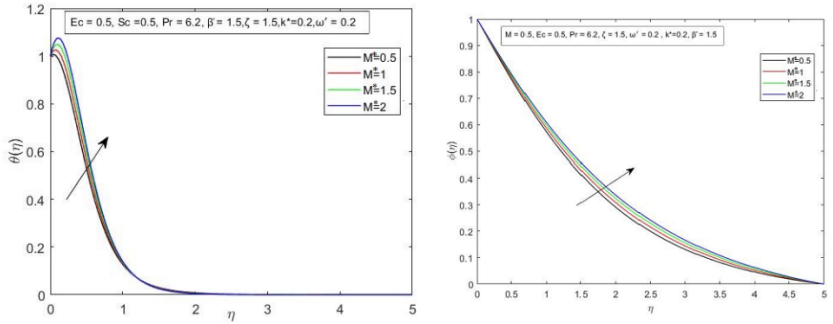

Figure 12. Impact of magnetic parameter on temperature and concentration profiles

Table 2. The numerical values of the local drag frictions in primary and transverse velocity directions and the heat transmission and mass transmit coefficients.

ω'	M^*	β	N_1^*	λ'	Sc	$-\left(1+\frac{1}{\beta'}\right)F''(0)$	$-\left(1+\frac{1}{\beta'}\right)G'(0)$	$-\theta'(0)$	$-\varphi'(0)$
0.2	0	1.5	0.5	0.5	0.5	1.576634	0.427427	1.870712	0.440973
	0.2					1.727631	0.380353	1.860252	0.431871
	0.4					1.871796	0.345165	1.850182	0.423028
	0.5					1.941233	0.330668	1.845306	0.418757
		0.5				1.941233	0.330668	1.845306	0.418757
		1				1.557119	0.274664	1.816289	0.392605
		1.5				1.409385	0.253036	1.80155	0.380588
		2				1.330321	0.241417	1.7925	0.373664
				6.5		2.509271	0.292722	1.808219	0.386121
				0		2.147491	0.318424	1.832336	0.408213
				0.5		1.807078	0.337982	1.853501	0.425064
				1		1.481167	0.354113	1.872698	0.439005
			0.5			1.498147	0.338127	1.871142	0.45017
			1			1.147264	0.358492	1.894246	0.465385
			1.5			0.811635	0.376036	1.915209	0.478728
			2			0.488162	0.391503	1.934507	0.490665
					0.5	1.717911	0.324062	1.855947	0.439844
					1	1.748305	0.319955	1.853188	0.656409
					1.5	1.766139	0.318003	1.851598	0.834714
					2	1.777684	0.316957	1.850589	0.986363
0.1						1.701912	0.163072	1.857367	0.441221
0.2						1.717911	0.324062	1.855947	0.439844
0.3						1.74381	0.481026	1.853621	0.437609
0.4						1.778524	0.632286	1.850496	0.434604

CONCLUSION

A spinning sheet subjected to a mixed convective 3D flow of Casson liquid was analysed in this study, and the following are the main characteristics of this inspection:

- Material parameter β improves velocity distributions, but temperature and concentration have the reverse effect.
- Thermal buoyancy λ^* and buoyancy ratio N_1^* have similar fluid velocity F' characteristics.
- When N_1^* grows, local Nusselt and Sherwood values improve for aiding flow ($\lambda^* > 0$). The skin friction coefficients decrease as N_1^* increases, whereas in the case of opposing flow (($\lambda^* < 0$), the reverse behaviour is observed. This is because of the reason that viscous forces are less effective when compared with buoyancy forces
- With increased concentration buoyancy factor N_1^*, skin friction coefficient declines, but transversal skin resistance number, local Nusselt, and Sherwood records decrease.
- The values of C_{fx}, and C_{fy} , local Nusselt and Sherwood numbers decrease for larger Casson fluid parameter values. Also, the local Nusselt number and the local Sherwood number reduced as the magnetic field parameter was increased.

Conflicts of Interest

The authors declare that there are no conflicts of interest.

Nomenclature and Abbreviations

u, v, w	*x, y, z components of velocity (ms^{-1})*	T_∞	*Free stream temperature (K)*
C_w	*Free stream concentration*	ρ	*Fluid density (kgm^{-3})*
g^-	*Gravitational force*	C_∞	*Uniform constant concentration*
T	*The temperature of the fluid (K)*	Ω'	*Angular velocity(ms^{-1})*
$\boldsymbol{D_m}$	*Mass diffusivity coefficient.*	B_0	*Applied magnetic field ($Wb\ m^{-2}$)*
M^*	*Magnetic Parameter*	α'	*Thermal diffusivity*
Cp	*Specific heat constant pressure ($Jkgk^{-1}$)*	ω'	*Rotational parameter*
C	*The concentration of the species*	β	*Casson Parameter*
T_w	*Surface temperature (K)*	Re_x	*Local Reynolds number*
v	*Kinematic viscosity (m^2s^{-1})*	Sc	*Schmidt number*
Pr	*Prandtl number*	μ	*Dynamic viscosity ($kgm^{-1}s^{-1}$)*
N_1^*	*concentration buoyancy parameter*	λ^*	*mixed convection parameter*
β_T	*Thermal expansion coefficient*	β_C	*Solutal expansion coefficient*

Abbreviations:

NNF	*Non- Newtonian Fluid*	*R. P*	*Rotational Parameter*
PVG	*Primary Velocity Gradient*	*SVG*	*Secondary Velocity Gradient*

REFERENCES

Ahmad, F., Waqas, H., Ayed, H., Hussain, S., Farooq, S., Khan, S.A and Almatroud, A.O. (2021). Numerical treatment with Lobatto-IIIa scheme magneto-thermo-natural convection flow of casson nanofluid (MoS2−Cu/SA) configured by a stretching cylinder in porous medium with multiple slips. *Case Studies in Thermal Engineering* **26.** https://doi.org/10.1016/j.csite.2021.101132

Ajibade, A.O., Umar, A.M and Kabir, T.M. (2021). An analytical study on effects of viscous dissipation and suction/injection on a steady mhd natural convection couette flow of heat generating/absorbing fluid. *Advances in Mechanical Engineering* **13**(5): 1–12. https://doi.org/10.1177/16878140211015862

Alhamaly, A.S., Khan, M., Shuja, S.Z., Yilbas, B.S and Al-Qahtani, H. (2021). Axisymmetric stagnation point flow on linearly stretching surfaces and heat transfer: Nanofluid with variable physical properties. *Case Studies in Thermal Engineering* **24**. https://doi.org/10.1016/j.csite.2021.100839

Ali, A., Farooq, H., Abbas, Z., Bukhari, Z and Fatima, A. (2020). Impact of Lorentz force on the pulsatile flow of a non-Newtonian Casson fluid in a constricted channel using Darcy's law: a numerical study. *Scientific Reports* **10**(1): 1–15. https://doi.org/10.1038/s41598-020-67685-0

Ali, B., Naqvi, R.A., Hussain, D., Aldossary, O.M and Hussain, S. (2020). Magnetic rotating flow of a hybrid nano-materials ag MoS2 and Go MoS2 in C2H6O2 H2O hybrid base fluid over an extending surface involving activation energy: Fe simulation. *Mathematics* **8**(10): 1–22. https://doi.org/10.3390/math8101730

Anuar, N.S., Bachok, N and Pop, I. (2020). Radiative hybrid nanofluid flow past a rotating permeable stretching/shrinking sheet. *International Journal of Numerical Methods for Heat and Fluid Flow* **31**(3): 914–932. https://doi.org/10.1108/HFF-03-2020-0149

Archana, M., Gireesha, B.J., Prasannakumara, B.C and Gorla, R.S.R. (2018). Influence of nonlinear thermal radiation on rotating flow of Casson nanofluid. *Nonlinear Engineering* **7**(2): 91–101. https://doi.org/10.1515/nleng-2017-0041

Besthapu, P., Haq, R.U., Bandari, S and Al-Mdallal, Q.M. (2019). Thermal radiation and slip effects on MHD stagnation point flow of non-Newtonian nanofluid over a convective stretching surface. *Neural Computing and Applications* **31**(1): 207–217. https://doi.org/10.1007/s00521-017-2992-x

Bilal Ashraf, M., Hayat, T and Alsaedi, A. (2017). Mixed convection flow of Casson fluid over a stretching sheet with convective boundary conditions and Hall effect. *Boundary Value Problems* **2017**(1). https://doi.org/10.1186/s13661-017-0869-7

Butt, A.S., Ali, A and Mehmood, A. (2015). Study of Flow and Heat Transfer on a Stretching Surface in a Rotating Casson Fluid. *Proceedings of the National Academy of Sciences India Section A - Physical Sciences* **85**(3): 421–426. https://doi.org/10.1007/s40010-015-0217-1

Gangaiah, T., Saidulu, N and Venkata Lakshmi, A. (2019). The influence of thermal radiation on mixed convection MHD flow of a casson nanofluid over an exponentially stretching sheet. *International Journal of Nanoscience and Nanotechnology* **15**(2): 83–98.

Ghosh, S and Mukhopadhyay, S. (2020). MHD mixed convection flow of a nanofluid past a stretching surface of variable thickness and vanishing nanoparticle flux. *Pramana - Journal of Physics* **94**(1). https://doi.org/10.1007/s12043-020-1924-y

Hussain, A., Haider, Q., Rehman, A., Ahmad, H., Baili, J., Aljahdaly, N.H and Hassan, A. (2021). A thermal conductivity model for hybrid heat and mass transfer investigation of single and multi-wall carbon nano-tubes flow induced by a spinning body. *Case Studies in Thermal Engineering* **28**: 101449. https://doi.org/10.1016/j.csite.2021.101449

Ibrahim, W. (2017). Passive control of nanoparticle of micropolar fluid past a stretching sheet with nanoparticles, convective boundary condition and second-order slip. *Proceedings of the Institution of Mechanical Engineers, Part E: Journal of Process Mechanical Engineering* **231**(4): 704–719. https://doi.org/10.1177/0954408916629907

Ijaz Khan, M., Nasir, T., Hayat, T., Khan, N.B and Alsaedi, A. (2020). Binary chemical reaction

with activation energy in rotating flow subject to nonlinear heat flux and heat source/sink. *Journal of Computational Design and Engineering* **7**(3): 279–286. https://doi.org/10.1093/jcde/qwaa023

Islam, T., Alam, M.N., Asjad, M.I., Parveen, N and Chu, Y.M. (2021). Heatline visualization of MHD natural convection heat transfer of nanofluid in a prismatic enclosure. *Scientific Reports* **11**(1): 1–18. https://doi.org/10.1038/s41598-021-89814-z

Malaver, M., Kasmaei, H.D., Khan, U and Zaib, Z. (2020). Mixed convective in an axisymmetric magneto flow owing to MoS2-GO hybrid nanoliquids in H2O based liquid through an upright cylinder with shape factor. Preprints 2020, 2020030301. DOI: 10.20944/preprints202003.0301.v1

Krishna, M.V., Ahammad, N.A and Chamkha, A.J. (2021). Radiative MHD flow of Casson hybrid nanofluid over an infinite exponentially accelerated vertical porous surface. *Case Studies in Thermal Engineering* **27**: 101229. https://doi.org/10.1016/j.csite.2021.101229

Lund, L.A., Omar, Z., Khan, I and Sherif, E.S.M. (2021a). Dual branches of mhd three-dimensional rotating flow of hybrid nanofluid on nonlinear shrinking sheet. *Computers, Materials and Continua* **66**(1): 127–139. https://doi.org/10.32604/cmc.2020.013120

Lund, L.A., Omar, Z., Raza, J and Khan, I. (2021b). Magnetohydrodynamic flow of Cu–Fe3O4/H2O hybrid nanofluid with effect of viscous dissipation: dual similarity solutions. *Journal of Thermal Analysis and Calorimetry* **143**(2), 915–927. https://doi.org/10.1007/S10973-020-09602-1

Mangathai, P and Reddy, B.R and Sidhartha, C. (2021). Unsteady MHD Williamson and Casson nano fluid flow in the presence of radiation and viscous dissipation. *Turkish Journal of Computer and Mathematics Education* **12**(13): 1036–1051.

Dash, R. K., Mehta, K.N and Jayaraman, G. (1996). Casson fluid flow in a pipe filled with a homogeneous porous medium. *International of Journal of Engineering Science* **34**(10): 1145–1156.

Nadeem, S and Saleem, S. (2014a). Mixed convection flow of Eyring-Powell fluid along a rotating cone. *Results in Physics* **4**: 54–62. https://doi.org/10.1016/j.rinp.2014.03.004

Nadeem, S and Saleem, S. (2014b). Theoretical investigation of MHD nanofluid flow over a rotating cone: an optimal solutions. *Information Sciences Letters* **3**(2): 55–62. https://doi.org/10.12785/isl/030203

Narender, G., Govardhan, K and Sarma, G.S. (2021). MHD Casson nanofluid past a stretching sheet with the effects of viscous dissipation, chemical reaction and heat source/sink. *Journal of Applied and Computational Mechanics* **7**(4): 2040–2048. https://doi.org/10.22055/JACM.2019.14804

Ouyang, C., Akhtar, R., Raja, M.A.Z., Touseef Sabir, M., Awais, M and Shoaib, M. (2020). Numerical treatment with Lobatto IIIA technique for radiative flow of MHD hybrid nanofluid (Al2O3-Cu/H2O) over a convectively heated stretchable rotating disk with velocity slip effects. *AIP Advances* **10**(5). https://doi.org/10.1063/1.5143937

Prathiba, A and Akavaram, V.L. (2022). Numerical investigation of a convective hybrid nanofluids around a rotating sheet. *Heat Transfer* **51**(4): 3353–3372. https://doi.org/10.1002/htj.22454

Qayyum, S., Khan, M.I., Hayat, T and Alsaedi, A. (2018). Comparative investigation of five nanoparticles in flow of viscous fluid with Joule heating and slip due to rotating disk. *Physica B: Condensed Matter* **534**: 173–183. https://doi.org/10.1016/j.physb.2018.01.044

Rajesh, V., Srilatha, M and Chamkha, A.J. (2020). Hydromagnetic effects on hybrid nanofluid (Cu–al2O3/Water) flow with convective heat transfer due to a stretching sheet. *Journal of Nanofluids* **9**(4): 293–301. https://doi.org/10.1166/JON.2020.1755

Raju, A.B.M.M and Mallikarjuna, B. (2019). Nonlinear convective rotating casson fluid flow over a radiated porous cone with rotation and variable properties. *Infokara Research* **8**(7): 75–92.

Rashid, S., Hayat, T., Qayyum, S., Ayub, M and Alsaedi, A. (2019). Three-dimensional rotating Darcy–Forchheimer flow with activation energy. *International Journal of Numerical Methods for Heat & Fluid Flow* **29**(3): 935–948. https://doi.org/10.1108/HFF-06-2018-0292

Reza, A.M., Chahal, R and Sharma, N. (2016). Radiation effect on MHD casson fluid flow over a

power-law stretching sheet with chemical reaction. *International Journal of Chemical, Molecular, Nuclear, Materials and Metallurgical Engineering* **3**(5): 46451.

Sahoo, A and Nandkeolyar, R. (2021). Entropy generation and dissipative heat transfer analysis of mixed convective hydromagnetic flow of a Casson nanofluid with thermal radiation and Hall current. *Scientific Reports* **11**(1). https://doi.org/10.1038/s41598-021-83124-0

Salahuddin, T., Siddique, N., Arshad, M and Tlili, I. (2020). Internal energy change and activation energy effects on Casson fluid. *AIP Advances* **10**(2). https://doi.org/10.1063/1.5140349

Satya Narayana, P.V., Tarakaramu, N., Sarojamma, G and Animasaun, I.L. (2021). Numerical simulation of nonlinear thermal radiation on the 3D flow of a couple stress casson nanofluid due to a stretching sheet. *Journal of Thermal Science and Engineering Applications* **13**(2): 1–10. https://doi.org/10.1115/1.4049425

Seghir-Ouali, S., Saury, D., Harmand, S., Phillipart, O and Laloy, D. (2006). Convective heat transfer inside a rotating cylinder with an axial air flow. *International Journal of Thermal Sciences* **45**(12): 1166–1178. https://doi.org/10.1016/j.ijthermalsci.2006.01.017

Senapati, M., Swain, K and Parida, S.K. (2020). Numerical analysis of three-dimensional MHD flow of Casson nanofluid past an exponentially stretching sheet. *Karbala International Journal of Modern Science* **6**(1): 93–102. https://doi.org/10.33640/2405-609X.1462

Shanker Seth, G and Kumar Mandal, P. (2018). Hydromagnetic rotating flow of Casson fluid in Darcy-Forchheimer porous medium. *MATEC Web of Conferences* **192**: 4–7. https://doi.org/10.1051/matecconf/201819202059

Shoaib, M., Raja, M. A.Z., Sabir, M.T., Awais, M., Islam, S., Shah, Z and Kumam, P. (2021). Numerical analysis of 3-D MHD hybrid nanofluid over a rotational disk in presence of thermal radiation with Joule heating and viscous dissipation effects using Lobatto IIIA technique. *Alexandria Engineering Journal* **60**(4): 3605–3619. https://doi.org/10.1016/j.aej.2021.02.015

Shoaib, M., Raja, M.A.Z., Sabir, M.T., Islam, S., Shah, Z., Kumam, P and Alrabaiah, H. (2020). Numerical investigation for rotating flow of MHD hybrid nanofluid with thermal radiation over a stretching sheet. *Scientific Reports* **10**(1): 1–15. https://doi.org/10.1038/s41598-020-75254-8

Uddin, I., Akhtar, R., Zhiyu, Z., Islam, S., Shoaib, M and Raja, M.A.Z. (2019). Numerical treatment for Darcy-Forchheimer flow of Sisko nanomaterial with Nonlinear thermal radiation by Lobatto IIIA technique. *Mathematical Problems in Engineering* **2019**. https://doi.org/10.1155/2019/8974572

Umar, M., Sabir, Z., Imran, A., Wahab, H. A., Shoaib, M and Raja, M.A.Z. (2020). The 3-D flow of casson nanofluid over a stretched sheet with chemical reactions, velocity slip, thermal radiation, and brownian motion. *Thermal Science* **24**(5): 2929–2939. https://doi.org/10.2298/TSCI190625339U

Vedavathi, N., Dharmaiah, G., Venkatadri, K and Gaffar, S.A. (2021). Numerical study of radiative non-Darcy nanofluid flow over a stretching sheet with a convective Nield conditions and energy activation. *Nonlinear Engineering* **10**(1): 159–176. https://doi.org/10.1515/nleng-2021-0012

Wang., C.Y. (1988). Stretching a surface in a rotating fluid. *Zeitschrift für Angewandte Mathematik und Physik* **39**(2): 177–185. https://doi.org/10.1007/BF00945764

Zaigham Zia, Q.M., Ullah, I., Waqas, M., Alsaedi, A and Hayat, T. (2018). Cross diffusion and exponential space dependent heat source impacts in radiated three-dimensional (3D) flow of Casson fluid by heated surface. *Results in Physics* **8**: 1275–1282. https://doi.org/10.1016/j.rinp.2018.01.001